Creating femtosecond-laser-hyperdoped silicon with a homogeneous doping profile

Yu-Ting Lin, Niall Mangan, Sophie Marbach, Tobias M. Schneider, Guoliang Deng, Shouhuan Zhou, Michael P. Brenner, and Eric Mazur

Citation: Applied Physics Letters **106**, 062105 (2015); doi: 10.1063/1.4907988
View online: http://dx.doi.org/10.1063/1.4907988
View Table of Contents: http://scitation.aip.org/content/aip/journal/apl/106/6?ver=pdfcov
Published by the AIP Publishing

Articles you may be interested in
Intermediate band conduction in femtosecond-laser hyperdoped silicon
Appl. Phys. Lett. **105**, 032103 (2014); 10.1063/1.4890618

Investigation of the sulfur doping profile in femtosecond-laser processed silicon
Appl. Phys. Lett. **102**, 202104 (2013); 10.1063/1.4807679

Electron backscatter diffraction on femtosecond laser sulfur hyperdoped silicon
Appl. Phys. Lett. **101**, 111911 (2012); 10.1063/1.4752454

Controlling dopant profiles in hyperdoped silicon by modifying dopant evaporation rates during pulsed laser melting
Appl. Phys. Lett. **100**, 112112 (2012); 10.1063/1.3695171

Reactivation of sub-bandgap absorption in chalcogen-hyperdoped silicon
Appl. Phys. Lett. **98**, 251905 (2011); 10.1063/1.3599450

Build and Run Simulation Apps with COMSOL 5.0
SEE HOW
COMSOL

This article is copyrighted as indicated in the article. Reuse of AIP content is subject to the terms at: http://scitation.aip.org/termsconditions. Downloaded to IP: 73.25.30.187 On: Wed, 11 Mar 2015 04:59:17

APPLIED PHYSICS LETTERS **106**, 062105 (2015)

Creating femtosecond-laser-hyperdoped silicon with a homogeneous doping profile

Yu-Ting Lin,[1] Niall Mangan,[1] Sophie Marbach,[1,3] Tobias M. Schneider,[4,5] Guoliang Deng,[1,6] Shouhuan Zhou,[6] Michael P. Brenner,[1] and Eric Mazur[1,2]
[1]*School of Engineering and Applied Sciences, Harvard University, Cambridge, Massachusetts 02138, USA*
[2]*Department of Physics, Harvard University, Cambridge, Massachusetts 02138, USA*
[3]*International Centre for Fundamental Physics, École Normale Supérieure, 75005 Paris, France*
[4]*Emergent Complexity in Physical Systems Lab (ECPS), École Polytechnique Fédérale de Lausanne, CH-1015 Lausanne, Switzerland*
[5]*Max Planck Institute for Dynamics and Self-Organization, Am Fassberg 17, 37077 Göttingen, Germany*
[6]*School of Electronics and Information Engineering, Sichuan University, Sichuan 610064, China*

(Received 8 December 2014; accepted 23 January 2015; published online 11 February 2015)

Femtosecond-laser hyperdoping of sulfur in silicon typically produces a concentration gradient that results in undesirable inhomogeneous material properties. Using a mathematical model of the doping process, we design a fabrication method consisting of a sequence of laser pulses with varying sulfur concentrations in the atmosphere, which produces hyperdoped silicon with a uniform concentration depth profile. Our measurements of the evolution of the concentration profiles with each laser pulse are consistent with our mathematical model of the doping mechanism, based on classical heat and solute diffusion coupled to the far-from-equilibrium dopant incorporation. The use of optimization methods opens an avenue for creating controllable hyperdoped materials on demand. © *2015 AIP Publishing LLC*.
[http://dx.doi.org/10.1063/1.4907988]

Optical and electronic properties of silicon are controlled by the concentration of dopants. Traditionally, the impurities are incorporated during the slow growth of silicon crystals from its melt, where dopant concentrations are limited to the equilibrium solubility limit in the solid. Nonequilibrium processes such as laser-hyperdoping can achieve much higher concentrations. Irradiating silicon with intense femtosecond-laser (fs-laser) pulses in a sulfur-containing atmosphere allows surpassing the equilibrium concentration limit by up to four orders of magnitude.[1] At sulfur concentrations of up to 1 at. %, the electronic band structure fundamentally changes. Overlapping sulfur donor states may create an additional metallic intermediate band, which enables two sub-band gap infrared (IR) photons to excite an electron from the valence band to the conduction band.[2–4] With its IR absorption capability, hyperdoped silicon is of interest for devices such as silicon-based IR detectors[5,6] and highly efficient photovoltaic cells that harvest additional energy from the sub-bang gap spectrum.[2,7,8]

Although laser-hyperdoping greatly expands the range of accessible dopant concentrations, it produces highly nonuniform dopant profiles in the material: the highest doping concentration sharply decays on a length scale of about a hundred nanometers from the surface into the bulk.[9] This nonuniformity produces undesirable variation in optical and electrical properties. Moreover, up until now, protocols for fs-laser doping have kept laser fluence and the sulfur-containing gas pressure in a fairly narrow range. This raises the question of whether it is possible to find a parameter range where the nonequilibrium doping produces a flat concentration profile up to a given depth.

In this letter, we present a doping process that achieves an almost flat concentration profile while preserving the crystallinity and the atomically smooth surface morphology. We use a mathematical model and experimental constraints to determine a fluence and gas pressure combination that maximizes the time for sulfur diffusion to flatten the concentration profile while avoiding solute rejection during solidification. Our mathematical model of the doping process is qualitatively consistent with experimental measurements.

The mathematical model of fs-laser induced hyperdoping[12] generalizes the previous models of nanosecond-laser (ns-laser) driven dopant incorporation.[10,11] We solve the equations of heat and solute transfer during melting and resolidification, when a silicon surface responds to the ultrafast laser energy deposition.[11] Unlike the ns-laser processes where the pulse duration is on the same time scale as the melting duration,[10,11] the fs-laser pulse deposits energy before the onset of any heat diffusion processes.[23] Therefore, we account for the energy deposition only in the initial condition for solving the heat equations. The model assumes that despite the extreme energy fluxes involved in the fs-laser treatment, the dopant incorporation mechanism is dominated by classical heat and solute diffusion coupled to the suppressed solute rejection at the moving liquid-solid boundary.[10] When a laser pulse of 100 fs and a fluence of 2.7 kJ/m^2 hits the silicon surface, the non-reflected part of the light is absorbed by the electronic-system. The silicon surface melts on a time scale much shorter than heat or solute diffusion and then develops a constant solidification velocity (Figure 1(a)). While the silicon is molten, adsorbed sulfur-containing molecules diffuse into the liquid surface and are incorporated when the surface cools and solidifies.[21] The key to achieve a nonequilibrium concentration is the extremely high intensity of the laser pulse of order 10^{12} W/m^2 causing nonlinear absorption of the energy in a very thin surface layer. A steep thermal gradient

 © 2015 AIP Publishing LLC

This article is copyrighted as indicated in the article. Reuse of AIP content is subject to the terms at: http://scitation.aip.org/termsconditions. Downloaded to IP: 73.25.30.187 On: Wed, 11 Mar 2015 04:59:17

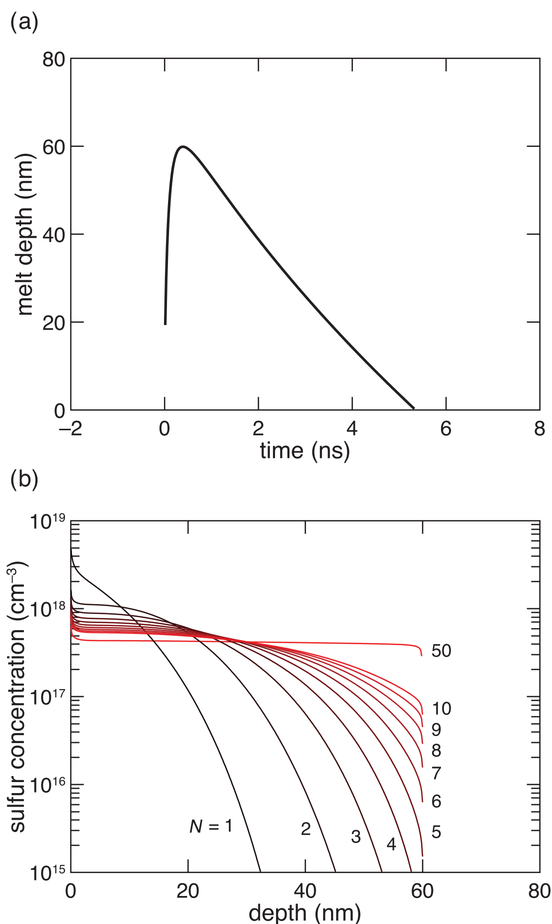

FIG. 1. (a) The simulated melt dynamics, and (b) the simulated doping profile evolution from 1 to 50 laser pulses at the same fluence. The sulfur is introduced as a sharp surface layer, meant to simulate an adsorbed layer, present only in the initial condition of the first laser pulse.

of 10^9 K/m results in a quick dissipation of the released latent heat during solidification. The phase change is driven to extreme nonequilibrium conditions and the resolidification velocity v is large compared to the diffusive velocity ($v_{DI} = 1$ m/s) at which sulfur ions can escape from the solid phase back to the liquid phase.[13] Consequently, instead of being rejected like salt from the slowly freezing seawater, the solute is 'trapped' in the solid, giving rise to greatly enhanced dopant concentrations. We estimate the partition coefficient, $K = (K_e + v/v_{DI})/(1 + v/v_{DI})$ to be 0.9, with the solute diffusive velocity of sulfur at the interface $v_{DI} = 1$ m/s and the equilibrium partition coefficient $K_e = 10^{-4}$.[10] Only 10% of the solute atoms in the solid phase escape back to the liquid phase. The doping concentration is several orders of magnitude beyond the thermodynamic equilibrium solubility limit (around 10^{16} cm^{-3}).[1,14]

We emphasize an important step in this presumed picture of hyperdoping: solute diffusion in the liquid phase during the doping process. If the dopants are truly transported diffusively in the liquid phase, we can utilize this mechanism to eliminate the concentration gradient by providing long enough diffusion time for the dopants to travel down the concentration gradient and pile up at the melt depth. Indeed, a thorough numerical search (see supplementary material[27]) for the optimum fluence and dopant precursor pressure sequence suggests the following design principle for fabricating a flat profile: introduce the dopants silicon with the first laser pulse and use subsequent pulses to diffuse the dopant out to the melt depth. We simulate the evolution of doping profiles over 50 laser pulses to illustrate the design principle (Figure 1(b)). In this simulation, a sulfur flux is present only for the first laser pulse, and the laser fluence is constant for each pulse. We also assume an ideal situation where all the dopants introduced in the first laser pulse remain in the silicon after subsequent laser pulses. Therefore, the sulfur dose, characterized by the area under the curve, is constant for each profile.

While the simulation suggests using as many laser pulses as possible to achieve a perfectly flat profile, we must take into account several limiting factors when designing the experiment. First of all, to study the doping profile with secondary ion mass spectrometry (SIMS), a flat surface is desirable for quantitative analysis. However, nanoscale surface periodic structures appear after many laser pulses, constraining the maximum number of laser pulses.[15,16] Second, the resolidification velocity increases with the decrease in fluence, leading to higher concentrations of lattice defects in the resolidified region. Eventually, the interface moves faster than the time required for atoms to diffuse and find a lattice site to sit in, resulting in amorphization. The transition velocity is approximately 15 m/s.[17] Finally, the laser fluence must be smaller than the ablation threshold.[18] Otherwise, significant material removal and unavoidable surface roughness complicate the SIMS measurements and analysis.

To achieve a flat profile, we maximize the integrated diffusion time for the dopants to transport down the concentration gradient and pile up at the melt depth. Therefore, we use a fluence that maximizes the number of laser pulses before the onset of surface texturing. We use a regeneratively amplified Ti:sapphire laser system to hyperdope silicon at a repetition rate of 100 Hz. The silicon cools to room temperature in less than 1 ms, so there is no thermal memory between laser pulses. The laser pulse has a wavelength centered at 810 nm and a pulse duration of 70 fs as measured with an autocorrelator. With the combination of a half waveplate and a polarizer, we tune the average pulse energy to 0.87 mJ and focus the pulse to a full-width at half-maximum of 1040 μm as measured with a CCD camera. The effective fluence is 2.7 kJ/m^2, which is above the melting threshold (1.5 kJ/m^2) and below the ablation threshold of silicon (3 kJ/m^2).[19]

Before hyperdoping, we pattern the silicon wafer (Boron-doped, resistivity = 7–14 Ω-cm) using a standard photolithography procedure and create circular mesas on the silicon surface with a reactive ion etch. These mesas, having a diameter of 800 μm and a height of 2 μm, serve for alignment purposes in the hyperdoping process and the SIMS measurements. We clean the patterned wafer with acetone, methanol, isopropanol, and water before placing it in a vacuum chamber. The chamber is pumped down to 10^{-6} Torr then back-filled with 730 Torr of SF_6. We use a mechanical shutter to control the number of laser pulses irradiating the silicon wafer and fabricate a set of 9 hyperdoped silicon samples labeled 1–9. The sample number corresponds to the total number of laser pulses delivered to the surface. For all the samples, we irradiate the first laser pulse in 730 Torr of SF_6. We perform all the subsequent pulses for sample number

This article is copyrighted as indicated in the article. Reuse of AIP content is subject to the terms at: http://scitation.aip.org/termsconditions. Downloaded to IP: 73.25.30.187 On: Wed, 11 Mar 2015 04:59:17

2–9 in vacuum (10^{-6} Torr). For example, sample 9 is irradiated by 1 laser pulse in SF_6 followed by 8 laser pulses in vacuum. We use Raman spectroscopy and optical profilometry to confirm that the surface is crystalline and atomically flat.

We then carry out SIMS measurements with a Cs ion beam of 6 keV at a current of 7 nA. We align the ion beam to the center of the laser-irradiated area. The ion beam is focused to a rectangular spot size of 150 μm $\times$ 200 μm while we collect only the center 15 μm $\times$ 30 μm of secondary ion signals by electronic gating, an area corresponding to less than 1% of fluence variation in the Gaussian pulse used for fabrication. We monitor ion channels including ^{29}Si, ^{32}S, ^{34}S, and ^{18}O. We use a standard sulfur sample (dose $= 1 \times 10^{14}$ cm^{-2}) made by ion implantation for calculating the relative sensitivity factor.

Figure 2 shows the experimentally measured sulfur concentration depth profiles. In the following context, we describe these profiles as "SIMS profiles" to distinguish them from the concentration profiles generated by the simulation. For clarity, we show only a subset of 5 of the SIMS samples. The SIMS profile for sample 1 demonstrates an exponential decay over depth. Upon subsequent pulses, the SIMS profile evolves deeper and deeper into the surface and the concentration gradient flattens out. Eventually, a plateau develops, and the SIMS profile for sample 9 has an abrupt cut-off at a depth of about 55 nm. We note that the data points within the first 6 nm of all curves are omitted because it takes time for SIMS to develop a stable drilling rate. The noise level is at about 10^{16} (cm^{-3}). In all samples, we observe an exponential tail with a decay rate of 10 nm/decade that is consistent with the SIMS mixing effect.[20] Cs ions cause this mixing effect by pushing sulfur ions into the sample rather than sputtering them off the surface. A SIMS concentration profile measured on a reference area that has not been irradiated by any laser pulses has a decaying oxygen signal with the same length scale coming from the native oxide covering the silicon surface.

Figure 3(a) shows a comparison between the numerical simulation and the experimental results for sample 1 and 9. While the SIMS profile for sample 1 follows similar exponential decay as the profile generated by the simulation, the SIMS profile for sample 9 is flatter than the simulated profile. Despite the discrepancy in slopes, the depths where the SIMS profile of sample 9 and the simulated profile cut off are within the measurement error in depth.[21] Figure 3(b) shows the sulfur dose, integration of the SIMS profile over depth, for each sample. Different from the assumed constant dose in the simulation, the dose monotonically decreases from 2×10^{12} to 1×10^{12} cm^{-2} after 9 laser pulses.

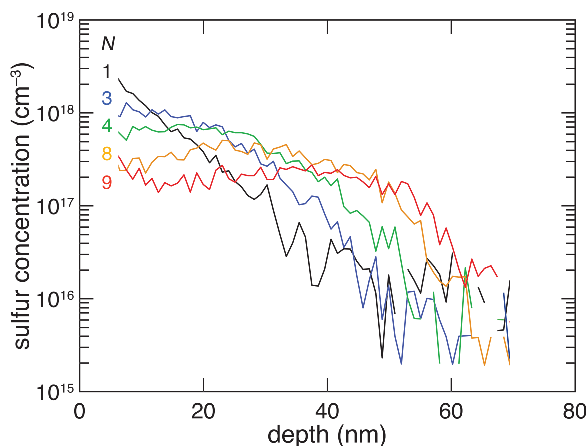

FIG. 2. Evolution of SIMS profiles of the hyperdoped samples from pulse 1 to 9. We select only these profiles for clarity. The profile changes from an exponential decay in the first pulse to a nearly flat profile in the 9th pulse.

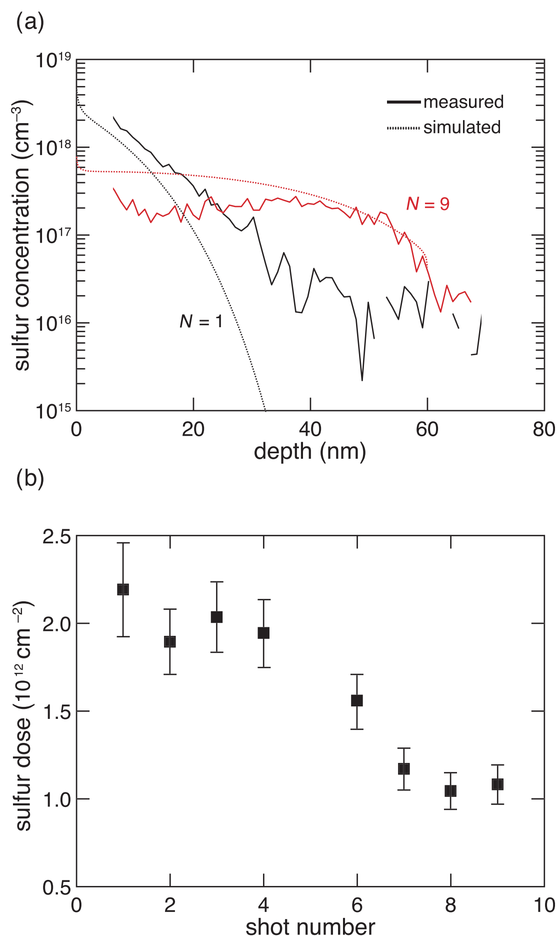

FIG. 3. (a) Comparison of the simulated (dashed) and measured SIMS profile (solid) for the samples 1 (black) and 9 (red). (b) Sulfur dose of each SIMS sample.

Our achievement of producing a flat concentration profile with the aid of a mathematical model demonstrates the feasibility of designing the doping profiles on demand. Our approach is distinct from previous hyperdoping processes where the dopant source is kept constant for every laser pulse.[9,22] Because the external dopant source is eliminated after the first laser pulse, we directly observe the dominating hyperdoping mechanism assumed in the numerical model by monitoring the change in doping profiles from pulse to pulse. While our previous study suggests a consistency between the experimental result and the simulation,[12,22] the validity of several assumptions made in the mathematical model requires closer examination. Our model adapts heterogeneous melting based on the fact that melting occurs on a time scale much faster than heat or solute diffusion.[23] The electron and phonon systems are under highly nonequilibrium conditions for the first few hundreds of picoseconds,[24] an effect not captured by our mathematical model. Despite this

This article is copyrighted as indicated in the article. Reuse of AIP content is subject to the terms at: http://scitation.aip.org/termsconditions. Downloaded to IP: 73.25.30.187 On: Wed, 11 Mar 2015 04:59:17

uncertainty in the real thermal evolution, our model uses the simulated melt dynamics—maximum melt depth and duration—determined in our previous study.[12,22] The only fitting parameter applied here is the total sulfur dose for the first laser pulse. The observed diffusive flattening from pulse to pulse in both the simulated and SIMS profiles therefore strongly suggests that the doping mechanism is dominated by the classical heat and solute diffusion coupled to the non-equilibrium solute trapping at the fast moving liquid/solid interface.

It is interesting to note that it takes fewer laser pulses to smooth out the sulfur concentration gradient than that predicted by the simulation (Figure 3(a)). Several factors may contribute to this discrepancy. The mathematical model assumes that all sulfur incorporated by the first laser pulse remains in silicon during subsequent laser pulses. However, the sulfur doses of the SIMS profiles show a decrease from 2×10^{12} to $1 \times 10^{12}\,\mathrm{cm}^{-2}$ with increasing laser pulses, indicating an outward flux of sulfur during doping. We believe that this arises from the presence of the native oxide layer on the surface of silicon, which is well known to serve as a diffusive barrier during doping. While the melting temperature of silicon oxide is at least 200 K higher than that of silicon, a laser pulse at $2.7\,\mathrm{kJ/m^2}$ could overheat the liquid silicon. Under elevated temperature, the silicon oxide could either evaporate or mix into the silicon melt. The absence of a uniform oxide layer allows sulfur to escape from the silicon. For example, an oxide layer has been used to control the dopant evaporation rate during ns-laser melting.[25] Another factor causing the discrepancy between experiment and simulation is that the finite resolidification velocity causes sulfur to be rejected from the solid phase and accumulate in front of the moving interface. Without an outward flux that releases the sulfur piling up near the end of the resolidification process, the simulation predicts a steep sulfur concentration slope at the surface that requires a longer integrated diffusion time to be erased.[22] As a result, the concentration gradient introduced in the first laser pulse is eliminated sooner than expected from the simulation.

Despite the experimental limitations that result in a 10-nm uncertainty in depth,[21] the abrupt drop in sulfur concentration in the SIMS curve for sample 9 is close to the predicted melt depth from the mathematical model. We believe this cut-off in the sulfur concentration indicates the actual melt depth and the dopants have reached the melt depth after 9 laser pulses. Given that the melt duration is about 5 ns obtained in our independent experiment reported elsewhere,[26] we estimate the diffusivity required to achieve a diffusion length of 55 nm during the doping process. The integrated diffusion length is approximately $L = \sqrt{(ND\tau)}$, where N is the number of laser pulses, D is the diffusivity of sulfur in liquid silicon, and τ is the melt duration. With $N = 9$, $\tau = 5\,\mathrm{ns}$,[26] and $L = 55\,\mathrm{nm}$, the $D = 6.7 \times 10^{-4}\,\mathrm{cm^2/s}$, which is comparable with the reported value of $2.7 \times 10^{-4}\,\mathrm{cm^2/s}$ in the literature[25] and used in our simulation. Therefore, we believe that we obtain a flat doping profile due to a combination of two effects: (1) a diffusion-driven decrease in concentration gradient over a relatively long melting time that results in the accumulation of sulfur at the melt depth, and (2) the escape of sulfur from the surface that facilitates the elimination of the concentration gradient.

In conclusion, we designed a simple recipe that effectively produces hyperdoped silicon of nearly constant doping concentrations over depth up to the melt depth. Additionally, our approach provides a direct confirmation of the underlying mechanism for fs-laser hyperdoping. Our work demonstrates optimization of a doping profile on demand and has a broader impact on the development of fs-laser hyperdoping using a gas-phase precursor.

Several people contributed to the work described in this paper. M.P.B., E.M., T.M.S., and N.M. conceived of the basic idea for this work. Y.-T.L. and G.D. designed and carried out the fabrication of hyperdoped silicon, while Y.-T.L. performed the SIMS measurements. S.M., N.M., and T.M.S. developed the theory. Y.-T.L., N.M., S.M., and T.M.S. analyzed the results. M.P.B. and E.M. supervised the research and the development of the manuscript. The author would like to thank Dr. Meng-Ju Sher and Dr. Mike Aziz for useful discussion. The research described in this paper was supported by NSF under the SOLAR Program, Grant No. DMR-0934480. Additionally, M.P.B. and N.M. gratefully acknowledge support from NSF-DMS1411694. M.P.B. is an investigator of the Simons Foundation.

[1] M. A. Sheehy, L. Winston, J. E. Carey, C. M. Friend, and E. Mazur, "Role of the background gas in the morphology and optical properties of laser-microstructured silicon," Chem. Mater. **17**(14), 3582–3586 (2005).
[2] A. Luque and A. Martí, "Increasing the efficiency of ideal solar cells by photon induced transitions at intermediate levels," Phys. Rev. Lett. **78**(26), 5014 (1997).
[3] M.-J. Sher, Y.-T. Lin, M. T. Winkler, E. Mazur, C. Pruner, and A. Asenbaum, "Mid-infrared absorptance of silicon hyperdoped with chalcogen via fs-laser irradiation," J. Appl. Phys. **113**, 063520 (2013).
[4] J. Olea, A. del Prado, D. Pastor, I. Mártil, and G. González-Díaz, "Sub-bandgap absorption in Ti implanted Si over the Mott limit," J. Appl. Phys. **109**(11), 113541 (2011).
[5] J. P. Mailoa, A. J. Akey, C. B. Simmons, D. Hutchinson, J. Mathews, J. T. Sullivan, D. Recht, M. T. Winkler, J. S. Williams, J. M. Warrender, P. D. Persans, M. J. Aziz, and T. Buonassisi, "Room-temperature sub-band gap optoelectronic response of hyperdoped silicon," Nat. Commun. **5**, 3011 (2014).
[6] J. E. Carey, C. H. Crouch, M. Shen, and E. Mazur, "Visible and near-infrared responsivity of femtosecond-laser microstructured silicon photodiodes," Opt. Lett. **30**(14), 1773–1775 (2005).
[7] D. Recht, M. J. Smith, S. Charnvanichborikarn, J. T. Sullivan, M. T. Winkler, J. Mathews, J. M. Warrender, T. Buonassisi, J. S. Williams, S. Gradečak, and M. J. Aziz, "Supersaturating silicon with transition metals by ion implantation and pulsed laser melting," J. Appl. Phys. **114**(12), 124903 (2013).
[8] S. Kontermann, T. Gimpel, A. L. Baumann, K.-M. Guenther, and W. Schade, "Laser processed black silicon for photovoltaic applications," Energy Procedia **27**, 390–395 (2012).
[9] M. T. Winkler, M.-J. Sher, Y.-T. Lin, M. J. Smith, H. Zhang, S. Gradečak, and E. Mazur, "Studying femtosecond-laser hyperdoping by controlling surface morphology," J. Appl. Phys. **111**, 093511 (2012).
[10] M. J. Aziz, "Model for solute redistribution during rapid solidification," J. Appl. Phys. **53**, 1158–1168 (1982).
[11] E. Landi, P. M. Carey, and T. W. Sigmon, "Numerical simulation of the gas immersion laser doping (GILD) process in silicon," IEEE Trans. Comput. Des. **7**(2), 205–214 (1988).
[12] N. Mangan, "Organization and diffusion in biological and material fabrication problems," Ph.D. dissertation (Harvard University, 2013).
[13] B. P. Bob, A. Kohno, S. Charnvanichborikarn, J. M. Warrender, I. Umezu, M. Tabbal, J. S. Williams, and M. J. Aziz, "Fabrication and subband gap optical properties of silicon supersaturated with chalcogens by ion implantation and pulsed laser melting," J. Appl. Phys. **107**(12), 123506 (2010).

This article is copyrighted as indicated in the article. Reuse of AIP content is subject to the terms at: http://scitation.aip.org/termsconditions. Downloaded to IP: 73.25.30.187 On: Wed, 11 Mar 2015 04:59:17

[14] H. Okamoto, *Phase Diagrams for Binary Alloys* (Mater. Park ASM Int., 2000).
[15] B. Tan and K. Venkatakrishnan, "A femtosecond laser-induced periodical surface structure on crystalline silicon," J. Micromech. Microeng. **16**(5), 1080–1085 (2006).
[16] T.-H. Her, R. J. Finlay, C. Wu, S. Deliwala, and E. Mazur, "Microstructuring of silicon with femtosecond laser pulses," Appl. Phys. Lett. **73**(12), 1673–1675 (1998).
[17] M. O. Thompson, J. W. Mayer, A. G. Cullis, H. C. Webber, N. G. Chew, J. M. Poate, and D. C. Jacobson, "Silicon melt, regrowth, and amorphization velocities during pulsed laser irradiation," Phys. Rev. Lett **50**, 896 (1983).
[18] K. Sokolowski-Tinten, J. Bialkowski, A. Cavalleri, D. von der Linde, A. Oparin, J. Meyer-ter-Vehn, and S. I. Anisimov, "Transient states of matter during short pulse laser ablation," Phys. Rev. Lett. **81**(1), 224 (1998).
[19] K. Sokolowski-Tinten, J. Bialkowski, M. Boing, A. Cavaller, and D. von der Linde, "Thermal and nonthermal melting of gallium arsenide after femtosecond laser excitation," Phys. Rev. B **58**(18), R11805 (1998).
[20] K. Wittmaack, "Beam-induced broadening effects in sputter depth profiling," Vacuum **34**(1–2), 119–137 (1984).
[21] M. A. Bassam, P. Parvin, B. Sajad, A. Moghimi, and H. Coster, "Measurement of optical and electrical properties of silicon microstructuring induced by ArF excimer laser at SF_6 atmosphere," Appl. Surf. Sci. **254**, 2621 (2008).
[22] M.-J. Sher, "Intermediate band properties of femtosecond-laser hyperdoped silicon," Ph.D. thesis (Harvard University, 2013).
[23] S. K. Sundaram and E. Mazur, "Inducing and probing non-thermal transitions in semiconductors using femtosecond laser pulses," Nat. Mater. **1**(4), 217–224 (2002).
[24] E. J. Yoffa, "Dynamics of dense laser-induced plasmas," Phys. Rev. B **21**(6), 2415 (1980).
[25] D. Recht, J. T. Sullivan, R. Reedy, T. Buonassisi, and M. J. Aziz, "Controlling dopant profiles in hyperdoped silicon by modifying dopant evaporation rates during pulsed laser melting," Appl. Phys. Lett. **100**(11), 112112 (2012).
[26] Y.-T. Lin, "Femtosecond-laser hyperdoping and texturing of silicon for photovoltaic applications," Ph.D. thesis (Harvard University, 2014).
[27] See supplementary material at http://dx.doi.org/10.1063/1.4907988 for details of the numerical method.

This article is copyrighted as indicated in the article. Reuse of AIP content is subject to the terms at: http://scitation.aip.org/termsconditions. Downloaded to IP: 73.25.30.187 On: Wed, 11 Mar 2015 04:59:17